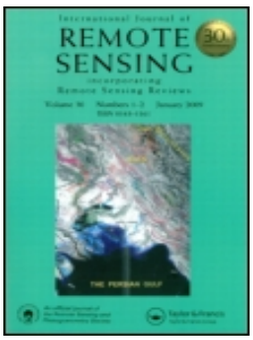

International Journal of Remote Sensing

ISSN: 0143-1161 (Print) 1366-5901 (Online) Journal homepage: https://www.tandfonline.com/loi/tres20

Assessment of forest cover in Russia by combining a wall-to-wall coarse-resolution land-cover map with a sample of 30 m resolution forest maps

Svyatoslav S. Bartalev, Ouns Kissiyar, Frédéric Achard, Sergey A. Bartalev & Dario Simonetti

To cite this article: Svyatoslav S. Bartalev, Ouns Kissiyar, Frédéric Achard, Sergey A. Bartalev & Dario Simonetti (2014) Assessment of forest cover in Russia by combining a wall-to-wall coarse-resolution land-cover map with a sample of 30 m resolution forest maps, International Journal of Remote Sensing, 35:7, 2671-2692, DOI: 10.1080/01431161.2014.883099

To link to this article: https://doi.org/10.1080/01431161.2014.883099

© 2014 The Author(s). Published by Taylor & Francis.

Published online: 27 Mar 2014.

Submit your article to this journal

Article views: 1209

View related articles

View Crossmark data

Citing articles: 5 View citing articles

Full Terms & Conditions of access and use can be found at
https://www.tandfonline.com/action/journalInformation?journalCode=tres20

International Journal of Remote Sensing, 2014
Vol. 35, No. 7, 2671–2692, http://dx.doi.org/10.1080/01431161.2014.883099

Taylor & Francis
Taylor & Francis Group

Assessment of forest cover in Russia by combining a wall-to-wall coarse-resolution land-cover map with a sample of 30 m resolution forest maps

Svyatoslav S. Bartalev[a], Ouns Kissiyar[a,b], Frédéric Achard[a]*, Sergey A. Bartalev[c], and Dario Simonetti[a,d]

[a]*Institute for Environment and Sustainability, Joint Research Centre of the European Commission, 21027 Ispra (VA), Italy;* [b]*AGIV, Agentschap voor Geografische Informatie Vlaanderen, 9000 Ghent, Belgium;* [c]*Terrestrial Ecosystems Monitoring Laboratory, Space Research Institute (IKI), Russian Academy of Sciences, 117997 Moscow, Russia;* [d]*Reggiani SpA, Institute for Environment and Sustainability, Joint Research Centre of the European Commission, I-21027 Ispra (VA), Italy*

(*Received 14 September 2012; accepted 24 June 2013*)

The process of gathering land-cover information has evolved significantly over the last decade (2000–2010). In addition to this, current technical infrastructure allows for more rapid and efficient processing of large multi-temporal image databases at continental scale. But whereas the data availability and processing capabilities have increased, the production of dedicated land-cover products with adequate accuracy is still a prerequisite for most users. Indeed, spatially explicit land-cover information is important and does not exist for many regions. Our study focuses on the boreal Eurasia region for which limited land-cover information is available at regional level.

The main aim of this paper is to demonstrate that a coarse-resolution land-cover map of the Russian Federation, the 'TerraNorte' map at 230 m × 230 m resolution for the year 2010, can be used in combination with a sample of reference forest maps at 30 m resolution to correctly assess forest cover in the Russian federation.

First, an accuracy assessment of the TerraNorte map is carried out through the use of reference forest maps derived from finer-resolution satellite imagery (Landsat Thematic Mapper (TM) sensor). A sample of 32 sites was selected for the detailed identification of forest cover from Landsat TM imagery. A methodological approach is developed to process and analyse the Landsat imagery based on unsupervised classification and cluster-based visual labelling. The resulting forest maps over the 32 sites are then used to evaluate the accuracy of the forest classes of the TerraNorte land-cover map. A regression analysis shows that the TerraNorte map produces satisfactory results for areas south of 65° N, whereas several forest classes in more northern areas have lower accuracy. This might be explained by the strong reflectance of background (i.e. non-tree) cover.

A forest area estimate is then derived by calibration of the TerraNorte Russian map using a sample of Landsat-derived reference maps (using a regression estimator approach). This estimate compares very well with the FAO FRA exercise for 2010 (1% difference for total forested area). We conclude that the TerraNorte map combined with finer-resolution reference maps can be used as a reliable spatial information layer for forest resources assessment over the Russian Federation at national scale.

*Corresponding author. Email: Frederic.Achard@jrc.ec.europa.eu

© 2014 The Author(s). Published by Taylor & Francis.
This is an Open Access article. Non-commercial re-use, distribution, and reproduction in any medium, provided the original work is properly attributed, cited, and is not altered, transformed, or built upon in any way, is permitted. The moral rights of the named author(s) have been asserted.

1. Introduction and objectives

Accurate, detailed, and regularly updated land-cover information has become paramount for addressing a range of important scientific questions relating to human activity with its ensuing ecological impact, in particular for Eurasian boreal ecosystems (Achard, Mollicone, and Stibig 2006; Achard et al. 2008). These scientific questions and their answers can have a direct impact on political decisions affecting (directly or indirectly) millions of people worldwide.

A number of global and continental land-cover mapping initiatives have already produced results at coarse scale. In the early 2000s, new global land-cover data sets were produced at a resolution of 1 km × 1 km from advanced Earth observation sensors (VEGETATION instrument on board the SPOT satellites, and the Moderate Resolution Imaging Spectro-radiometer, or MODIS, on board the Terra and Aqua platforms). These products, GLC-2000 (Bartholomé and Belward 2005) and MODIS Global Land-cover (Friedl, McIver, and Hodges 2002), allowed for a spatial and thematic refinement of previous global maps owing to enhanced sensor calibration, increased spectral, spatial, and temporal resolution, as well as improved classification algorithms. More recently, new global land-cover data sets at finer spatial resolution (from 250 m × 250 m to 500 m × 500 m) were generated from Terra-MODIS or ENVISAT-MERIS sensors. The two key products at this scale are the Vegetation Continuous Fields (VCF) product and the GlobCover map. The MODIS-derived VCF product depicts sub-pixel vegetation cover traits at a spatial resolution of 500 m × 500 m (Hansen et al. 2005). A more recent version (2005) of the MODIS Global Land-cover product has also been generated with substantial differences arising from increased spatial resolution (500 m × 500 m) and changes in the input data and classification algorithm (Friedl, Sulla-Menashe, and Tan 2010). The 'GlobCover' initiative produced a global land-cover map using the 300 m resolution mode from the MERIS sensor on board the ENVISAT satellite (Arino et al. 2008) acquired during 2005. The GlobCover global land-cover map has complemented previous global products and other existing comparable continental products with improvement in terms of spatial resolution.

As a part of the GLC2000 project, a first land-cover map for boreal Eurasia has been produced based on SPOT-VEGETATION data for 2000 at 1.15 km spatial resolution (Bartalev et al. 2003). This map is one of the most widely used land-cover products for environmental research studies and applications at the sub-continental level for this region. More recently an automated land-cover mapping method based on a new Locally Adaptive Global Mapping Algorithm (LAGMA) has been developed within the framework of the TerraNorte project and has been used for land-cover mapping over Russia (Uvarov and Bartalev 2010). This method allows the use of increased sensor capabilities (finer spatial resolution and improved spectral characteristics) to derive continental to global land-cover products.

This study was initiated as part of the PROBA-V Preparatory Programme. The Project for On-Board Autonomy (PROBA) started as a technology demonstration mission of the European Space Agency (ESA) with the aim of using and demonstrating automatic functions, both onboard and in the mission ground segment. PROBA-V, where V stands for Vegetation, was built to redress the data gap that occurred when the SPOT 4 and SPOT 5 satellites carrying the VEGETATION instruments came to the end of their operational missions at the end of 2012. PROBA-V will thus provide data continuity to the VEGETATION user community until the launch of the first Sentinel 3 satellite (2015). This study is part of the TerraNorte project within the PROBA-V Preparatory Programme. The TerraNorte project aimed at evaluating the impact of enhanced-spatial resolution data for boreal land-cover mapping with a geographical focus on Russia and a thematic focus

on forests. The future PROBA-V mission will fly a reduced-mass version of the VEGETATION instrument, to provide a daily overview of the global vegetation status. An improvement in the performance of the PROBA-V sensor was sought with enhanced spatial and spectral resolutions (ESA 2012). The PROBA-V TerraNorte project used MODIS imagery at 230 m resolution (as a proxy for the PROBA-V mission) and produced as the main output a new land-cover map of the Russian Federation for the year 2010 at about 300 m resolution. The main aim of our paper is to evaluate the accuracy of this recent coarse continental land-cover map and to assess its potential use for forest resource assessment at national scale. Medium-resolution forest maps are used over sample sites as reference maps (derived from Landsat TM imagery).

2. Methodology

2.1. Data sets

2.1.1. TerraNorte land-cover map of Russia

Bartalev et al. (2012) evaluated the impact of the enhanced spatial resolution of the future PROBA-V sensor (300 m in VNIR channels at swath edge) *versus* the VEGETATION sensor (1.15 km) for boreal land-cover mapping over Russia, with a thematic focus on forests. MODIS data were used as a proxy for the PROBA-V mission due to similarities in spectral channels, spatial resolution, and observation frequency for regions at high latitude (between 35° N and 75° N). An automated method (Bartalev et al. 2011) has been used to map the vegetation cover using MODIS data. This method involves the generation of multi-annual time-series of surface reflectance data, which are used for land-cover type classification based on a locally adaptive algorithm (Uvarov and Bartalev 2010). This method has been used for producing time-series of annual land-cover maps over Russia from 2000. For this specific study we used the annual land-cover map for the year 2010.

The TerraNorte map legend consists of 22 thematic classes, including 18 vegetation classes described through their life forms, leaf type, and phenology (see Table 1).

2.1.2. Landsat imagery

We consider Landsat TM imagery as appropriate data for producing reference vegetation maps to assess the accuracy of the continental map (Jensen 1996). A sample consisting of 32 units of 20 km × 20 km size was selected for the detailed identification of forest cover from Landsat TM imagery (see Figure 1). These sample sites were selected from the systematic sample database of the global remote sensing survey of the FAO (Beuchle et al. 2011; FAO and JRC 2012). Stratified sampling has been demonstrated to be a robust approach for forest cover monitoring (Richards, Gallego, and Achard 2000; Stehman 2001; Stehman et al. 2003; Stehman et al. 2011). However our sub-sample (of the systematic sample) was selected empirically in order to incorporate challenging areas from the point of view of land-cover mapping within the TerraNorte map and to represent the large latitudinal, longitudinal, and climatic heterogeneity that characterizes the forested landscape across the Russian Federation. The TerraNorte map was derived from MODIS decadal mosaics over a period of 12 years. From these MODIS mosaics a number of regions were identified as being temporally unstable (i.e. between different years in the 12-year period) from a land-cover perspective. These regions were the most challenging areas for the land-cover classification process of the TerraNorte map, which can probably be explained by their spatial or temporal land-cover heterogeneity. We

Table 1. Land-cover legend for 30-m resolution maps.

	Name of land-cover class	Description with dominant/subdominant species
1	Evergreen dark needleleaf forest (ED)	Forest ecosystems consisting of spruce (Picea), fir (Abies), and Siberian pine (*Pinus sibirica*) for at least 80% of the forest canopy
2	Evergreen light needleleaf forest (EL)	Forest ecosystems consisting of pine (*P. sylvestris*) for at least 80% of the forest canopy
3	Deciduous broadleaf forest (Brd)	Forest ecosystems consisting of birch (Betula), aspen (*Populus tremula*), oak (Quercus), linden (Tilia), ash (Fraxinus), maple (Acer), and some other deciduous broadleaf tree species for at least 80% of the forest canopy
4	Mixed needleleaf majority forest (MNM)	Forest ecosystems consisting of the evergreen needleleaf tree species for 60% to 80% and the deciduous broadleaf tree species for 20% to 40% of the forest canopy
5	Mixed forest (M)	Proportions of the evergreen needleleaf and the deciduous broadleaf tree species in the forest canopy are approximately equal (40% to 60%)
6	Mixed broadleaf majority forest (MBM)	Forest ecosystems consisting of the deciduous broadleaf species for 60% to 80% and the evergreen needleleaf species for 20% to 40% of the forest canopy
7	Deciduous needleleaf forest (DN)	Forest ecosystems consisting of larch (Larix) for at least 80% of the forest canopy
8	Sparse deciduous needleleaf forest (SD)	Single trees or open stands of larch (Larix) with density of canopy below 20%
9	Peatlands (Ptlnd)	Permanent mixture of water and vegetation: Sphagnum moss and lichens, or rushes and sedges are dominant. Sometimes sparse tree canopy (up to 20%) can be found.
10	Recent burns	Burn scars <5 years old. May contain dead trees, some pioneer vegetation types may be present
11	Water bodies	Open water bodies including seas, lakes, reservoirs, and rivers
12	Other land	Lands having a vegetation canopy coverage smaller than 20%
13	Shrubs	Shrublands or low trees (height is less than 5 m more than 50 cm)

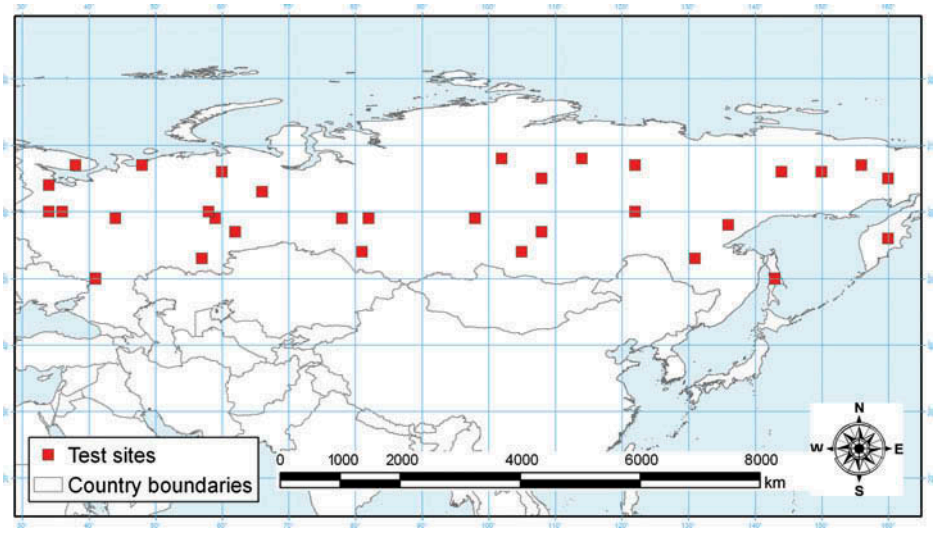

Figure 1. Location of the 32 test sites.

selected all sites of the full FAO-FRA 2010 systematic sample that fell within these challenging areas: this selection led to 32 sample sites.

The 32 sample sites include representative areas of all classes of the TerraNorte legend. In the TerraNorte map the classes that correspond to Other Land and Shrubs comprise 42.9% of the territory. The preponderance of the classes Other Land and Shrubs is attenuated in the coverage of the 32 sample sites to a mere 17.3%, due to their higher temporal stability compared with forest classes. Taken separately, the cover proportions of the forest classes are very similar for the whole TerraNorte map and for the set of 32 sample sites. All Broadleaf forests cover 14% of the TerraNorte map and 13.3% in the 32 selected sample sites, when the cover proportions for All Needleleaf forest classes are 63.2% and 61.6%, respectively.

For each sample site, satellite imagery from the Landsat TM sensor for the years 1990 and 2010, and from the Enhanced Thematic Mapper (ETM +) sensor for around the year 2000, was screened from the USGS database (http://glovis.usgs.gov/) (Beuchle et al. 2011). The most suitable images were selected considering the following criteria: acquisition year as close as possible to three reference years (1990, 2000, and 2010); and limiting the acquisition period from June to August, because during this period the spectral appearance of boreal forests is stable and is less influenced by the effects of growth, shade, or leaf drop, or by snow (Bucha and Stibig 2008). The main reason for using a time-series of satellite imagery for each site lies in the greater depth of information provided for the visual interpretation phase in comparison with using one single image. Furthermore it is intended to use the temporal series for change assessment in a future phase, similarly to a study carried out over South America (Eva et al. 2012).

A set of 32 Landsat images was selected for each year of analysis. In total we thus processed a set of 96 Landsat images. For this, a robust methodological approach needed to be developed. The available imagery was first pre-processed in a standardized manner to allow for accurate information extraction from the time-series. As described by Bodart et al. (2011), each image was converted to top-of-atmosphere reflectance (ToAR) and, where appropriate, haze correction was applied. As a final step we applied relative normalization to all images from one site by using the Dark Object Subtraction (DOS) method (Chavez 1996).

2.2. *Land-cover mapping from Landsat TM imagery*

2.2.1. *Unsupervised cluster classification*

For each of the 32 sites, one multi-temporal Landsat imagery stack is created. The Red, NIR, and SWIR bands (0.63–0.69, 0.75–0.9, and 1.55–1.75 μm, respectively) of the selected images for three reference years (1990, 2000, and 2010) were combined into one image stack per site.

The unsupervised Iterative Self-Organizing Data Analysis Technique (ISODATA) algorithm was selected to classify the images into 70 automatic clusters. This algorithm relies on pixel-based spectral statistics and incorporates no prior knowledge of the characteristics of the themes under study. The benefit of applying unsupervised classification methods is to automatically convert spectral image data into spatial clusters, which can then be used for land-cover classification (Xie, Sha, and Yu 2008). This approach has been proven to be effective and well suited to forest species classification (Reese et al. 2002), and has also been applied for other global land-cover classifications (Hansen and Reed 2000).

To label the clusters as land-cover classes, an interactive expert interpretation step was used as the final step in the land-cover mapping process.

2.2.2. Land-cover legend

One key objective for the design of the legend to be used for the Landsat-derived land-cover maps was that it had to be compatible with the legend of the TerraNorte land-cover map in order to allow a straightforward comparison between these maps at two different resolutions.

Bartalev (2006) showed that Landsat TM or ETM+ imagery allows the identification of a few forest classes through visual interpretation: Evergreen dark needleleaf forest, Deciduous broadleaf forest, and Evergreen light needleleaf forest. For the purpose of our study we defined 13 land-cover classes (Table 1). Given the focus on forests, special attention was devoted to the differentiation between eight specific forest cover types.

The resulting Landsat land-cover maps at 30 m × 30 m are then resampled to 230 m × 230 m resolution using a land-cover majority filter. This method was chosen as it most closely reproduced the outcome of the classification process applied to medium-scale satellite imagery. This is reflected in the correlation coefficients reported in Table 2. The correlation between the Landsat-based classification and resampled classification at 230 m only drops below 0.99 two cases (Recent burns class with 0.94 and the Evergreen light needleleaf forest with 0.96). This data set of 230 m × 230 m resolution was used to assess the impact of the spatial resolution of the reference land-cover products on the assessment of the accuracy of the continental land-cover map.

2.3. Accuracy assessment

Many studies have compared global land-cover data sets produced from different data sources at various spatial scales, using various classification systems and methodologies (Hansen and Reed 2000; Giri, Zhu, and Reed 2005; McCallum et al. 2006; Friedl, Sulla-Menashe, and Tan 2010; Broich et al. 2011; Lu et al. 2011). Any land-cover product should be (objectively) verified and this evaluation must be provided to users so that informed decisions can be made on whether and how the products can be used. A

Table 2. Coefficients of correlation between TerraNorte map (TN), Landsat-derived maps at 30 m resolution (LS 30 m), and Landsat-derived maps at 230 m resolution (LS 230 m).

Map combinations Land-cover classes	TN – LS 30 m	TN – LS 230 m	LS 30 m – LS 230 m
All Forests	0.862	0.861	0.989
All broadleaf forests	0.660	0.678	0.997
Deciduous broadleaf	0.628	0.632	0.998
Mixed broadleaf majority 80%	0.080	0.090	0.996
All needleleaf forests	0.821	0.849	0.993
Deciduous needleleaf forest	0.876	0.879	0.999
Sparse deciduous	0.682	0.682	0.999
Evergreen dark needleleaf forest	0.874	0.834	0.995
Evergreen light needleleaf forest	0.891	0.880	0.963
Mixed needleleaf majority 80%	0.704	0.696	0.997
Mixed forests	0.355	0.364	0.990
Other land	0.930	0.927	0.995
Peatlands	0.903	0.904	1.000
Recent burns	0.667	0.644	0.943
Shrubs	0.595	0.605	0.997
Water bodies	0.890	0.882	1.000

vegetation map derived from image classification is considered accurate if it provides a true representation of the region it portrays (Foody 2002; Weber 2006). Accuracy assessments are employed to indicate the degree of 'correctness' of the map compared to the reality in the field. Congalton (1994) describes four types of accuracy assessment with increasing level of detail and certainty:

(1) visual inspection of maps;
(2) comparison of areal extent of the classes in the derived maps with ground data or a reference data set;
(3) comparison of class labels in the thematic map with the ground data for the same locations;
(4) the best level includes further refinements on the basis of the third level. Most often a confusion or error matrix is used.

Although it is agreed that accuracy assessment is important to qualify the results of image classification, it is probably impossible to specify a single, all-purpose measure for assessing classification accuracy (Xie, Sha, and Yu 2008). We therefore decided to report more closely on the second, third, and fourth levels of accuracy assessment as described by Congalton (1994).

For accuracy assessment an ideal reference data set would consist of extensive field data, but given the extent of our study area (Russian Federation), such field data are difficult to collect for logistical reasons. For the purposes of our study we consider our sample data set of forest cover maps at 30 m resolution as surrogate for field data (Foody 2010) against which the TerraNorte map is assessed.

2.4. *Statistical parameters used for accuracy assessment*

Several statistical methods have been used for evaluation of the agreement/disagreement between the TerraNorte land-cover map and the Landsat-derived reference maps. These methods are briefly described hereafter alongside the calculations used.

2.4.1. *Pearson correlation coefficient*

The Pearson correlation coefficient measures the (linear) correlation between two variables x and y and is typically denoted as r. It is widely used as a measure of strength of (linear) dependence between two variables.

This correlation coefficient differs from the R-squared coefficient (R^2), which is also reported in several figures in this paper. The R^2 value can be interpreted as the proportion of the variance in y attributable to the variance in x. It is, in other words, the squared value of the previously calculated correlation coefficient.

2.4.2. *Linear regression*

A linear regression models the relationship between a dependent variable y and one (or more) explanatory variables x. Linear regressions can be used to fit a predictive model to an observed data set. The standard error is calculated to infer confidence intervals for the estimations, as this predicts the level of error in the predicted value of y for an individual x value.

2.4.3. Confusion matrix evaluation

A confusion matrix describes fitness between the derived classes and the reference data through measures such as overall accuracy and kappa coefficient. Additionally, a variety of other measures can be derived from the confusion matrix (e.g. the level of agreement, the expected fraction of agreement, and the maximum fraction *f* agreement). The level of agreement between two maps can be expressed in a single-digit kappa, based on the confusion matrix (or contingency table). This matrix shows how the distribution of classes in Map A differs from that of Map B. We used three statistical parameters derived from the confusion matrices:

$P(A)$, the fraction of agreement, calculated according to Equation (1):

$$P(A) = \sum_{i=1}^{c} p_{ii}, \tag{1}$$

where p_{ii} is the proportion of pixels of class i in classification A and class i in the reference data. $P(E)$, the expected fraction of agreement subject to the observed distribution, calculated according to Equation (2):

$$P(E) = \sum_{i=1}^{c} p_{i_T} \times P_{T_i}, \tag{2}$$

where p_{i_T} is the proportion of pixels of class i in Map A, and P_{T_i} is the proportion of pixels of class i in Map B $P(\max)$, the maximum fraction of agreement subject to the observed distribution. This is the maximum agreement that could be attained if the location of the cells in one map was to be rearranged. It is calculated according to Equation (3):

$$P(\max) = \sum_{i=1}^{c} \min(p_{i_T}, P_{T_i}). \tag{3}$$

These parameters are then used to calculate two different versions of the kappa coefficient – the standard value and the adapted-to-location value.

The kappa coefficient reports the proportion of agreement $P(A)$ after removal of the random chance agreement $P(E)$. It varies between 1 (perfect agreement) and 0 (randomly arranged cells), and can be calculated by the following Equation (4):

$$\kappa = \frac{P(A) - P(E)}{1 - P(E)}. \tag{4}$$

However, the kappa coefficient explains only part of the cell-by-cell agreement between two maps. Pontius (2000) introduced two statistical parameters to separate the quantification error from the location error, which are both included within kappa. The kappa location coefficient (κ_{loc}) compares the actual success rate to the expected success rate relative to the maximum success rate given a constant number of cells for each category. The maximum value for κ_{loc} is 1, with no minimal value. The advantage of κ_{loc} is that it is independent from the total number of cells in each category:

$$\kappa_{\text{loc}} = \frac{P(A) - P(E)}{P(\max) - P(E)}. \tag{5}$$

3. Results

3.1. Comparison of areal extent of classes

A quick initial visual comparison was made between the Landsat-derived reference maps and the TerraNorte map (Figure 2). This comparison was deemed to show agreement sufficiently good to warrant further statistical inquiry. As suggested by several authors (Giri, Zhu, and Reed 2005; Broich et al. 2011), we then proceeded to a more detailed comparison by relating the total area per class in the TerraNorte classification to the summed area in the reference data set. Correlation tables were produced for the different land-cover classes summed over all sites and individually for all 32 sites. For a given land-cover class the correlation between the class areas within each classification was calculated according to Pearson's correlation coefficient (Figure 3).

Table 2 shows a high correlation between the Landsat classification at 30 m resolution and the generalization at 230 m resolution, which is not really surprising but had to be

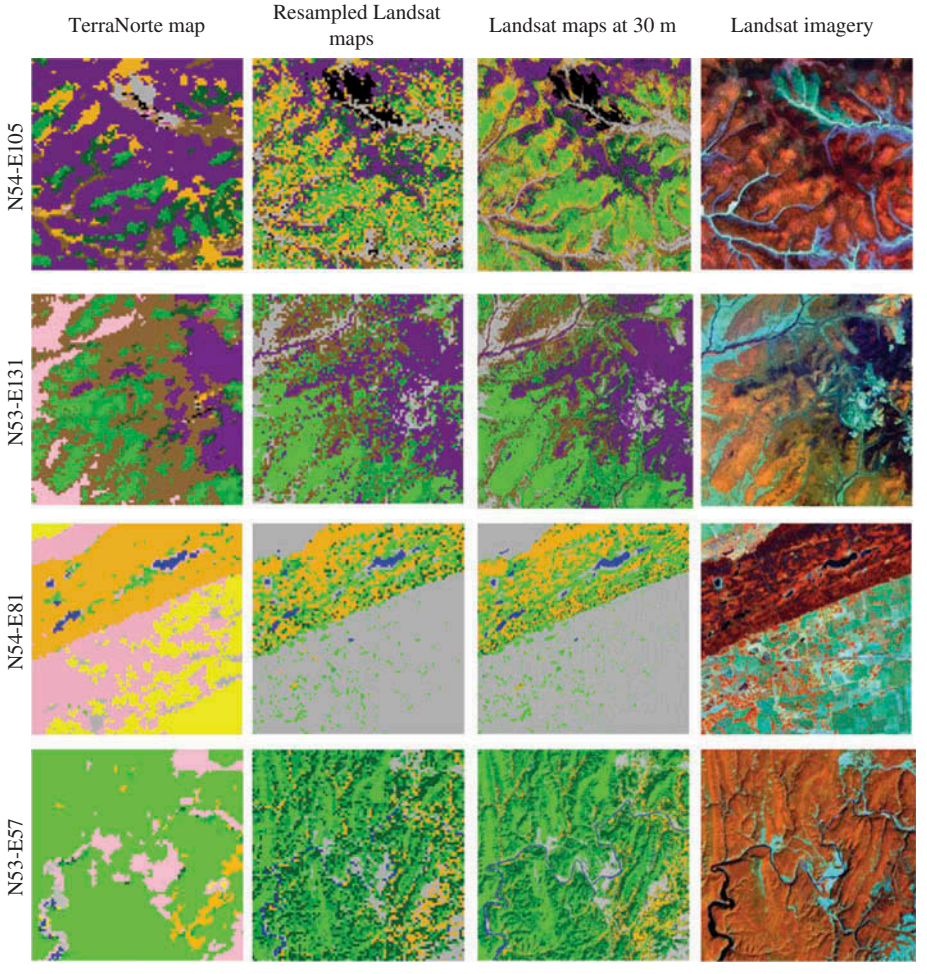

Figure 2. TerraNorte map at 230 m resolution, Landsat-derived maps resampled at 230 m resolution, Landsat-derived maps at 30 m resolution, and Landsat imagery at 30 m resolution for four sample sites. Each sample site measures 20 km × 20 km, N is at the top of the Figure. The location of the centre point of each box is indicated in the left margin.

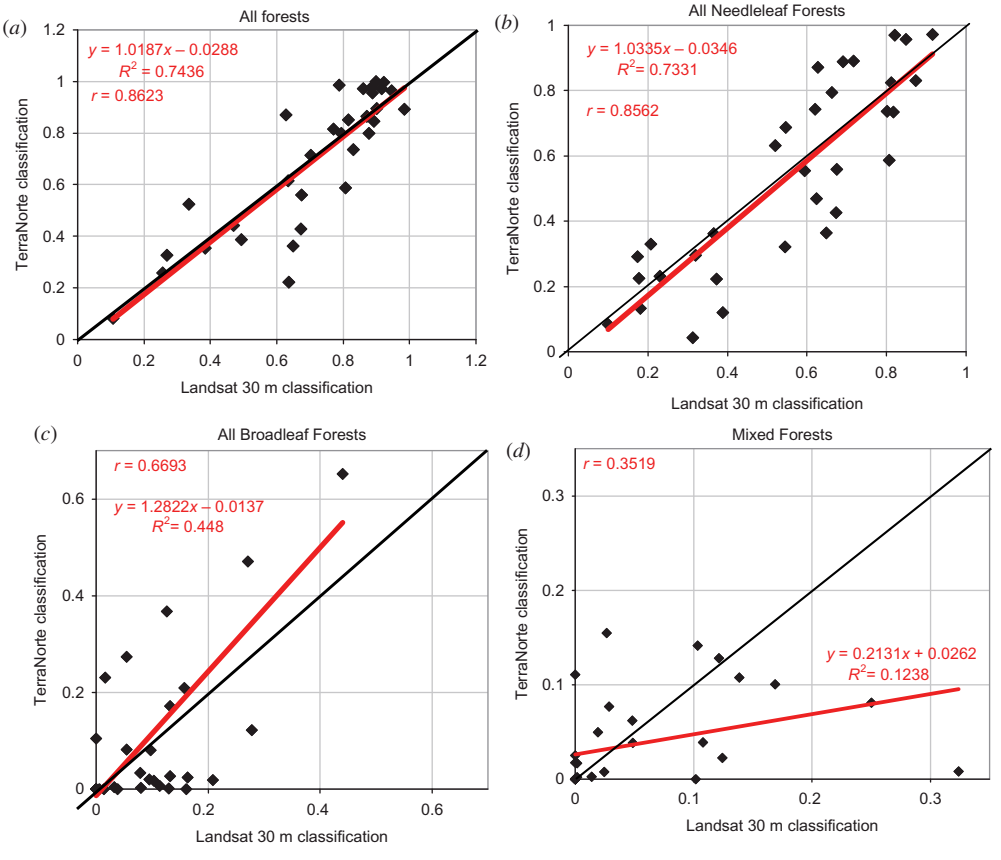

Figure 3. Regressions of class area between 30 m resolution maps and TerraNorte map for the sample sites for: (*a*) sum of all forest classes; (*b*) all needleleaf forests (evergreen dark and light needleleaf, deciduous needleleaf, sparse deciduous, and mixed needleleaf majority); (*c*) all broadleaf forests (deciduous broadleaf and mixed broadleaf majority); (*d*) mixed forests.

verified. This is also reflected in the very similar correlations between the TerraNorte map and either the Landsat-derived maps at 30 m resolution or the Landsat-derived resampled maps at 230 m resolution.

Correlation coefficients between the TerraNorte and the Landsat 30 m maps have generally high values. However, two land-cover classes demonstrate almost no correlation: Mixed forests (0.355) and Mixed broadleaf majority 80% (0.080). Even though the definition of these classes with a mixed composition may imply more errors in their delineation, the absence of correlation is surprising.

The correlation coefficients between the TerraNorte map and the Landsat-derived maps at 30 m resolution per individual site show a high overall agreement (Table 3). However, there are significant differences for four sites, where the correlation coefficients are below 0.7. For seven other sites the correlation coefficients are between 0.73 and 0.8, which is good but warranted closer inspection. For the remaining 21 sites the correlation coefficients are higher than 0.8.

When looking at the differences in regard to forest areas per site between the TerraNorte map and the Landsat 30 m classification, it appears that such differences significantly increase above 65° N (Figure 4). Whereas the average difference (relative

Table 3. Coefficients of correlation between TerraNorte map and 30 m resolution maps by sample site.

Box No.	Latitude/longitude	Correlation
1	50° N 41° E	1.00
2	50° N 143° E	0.89
3	53° N 57° E	0.48
4	53° N 131° E	0.66
5	54° N 81° E	0.95
6	54° N 105° E	0.87
7	56° N 160° E	0.74
8	57° N 62° E	0.95
9	57° N 108° E	0.84
10	58° N 136° E	0.77
11	59° N 44° E	0.77
12	59° N 59° E	0.95
13	59° N 78° E	0.86
14	59° N 82° E	0.95
15	59° N 98° E	0.77
16	60° N 34° E	0.50
17	60° N 36° E	0.78
18	60° N 58° E	0.82
19	60° N 122° E	0.83
20	63° N 66° E	0.86
21	64° N 34° E	0.98
22	65° N 108° E	0.95
23	65° N 160° E	0.90
24	66° N 60° E	0.86
25	66° N 144° E	0.84
26	66° N 150° E	0.61
27	67° N 38° E	0.75
28	67° N 48° E	0.76
29	67° N 122° E	0.81
30	67° N 156° E	0.86
31	68° N 102° E	0.93
32	68° N 114° E	0.99

percentage compared to Landsat map forest area) below 65° N is –2% (with standard deviation (SD) of 10%), this increases to 10% (SD 36%) above 65° N. Although only 11 among the 32 sample sites are located above 65° N, this clear trend prompted us to recalculate the correlation coefficients for two separate regions by splitting the Russian territory into two areas – above and below 65° N. Correlation coefficients for individual land-cover classes become closer to 1 for the southern region whereas they decrease for the northern region, and no correlation then exists for Broadleaf forests, Mixed forests, and other land classes (Table 4). The classes Shrubs, Recent burns, and Sparse deciduous are also heavily affected by a loss of correlation in the northern region.

3.2. Spatial agreement between maps

For the third and fourth levels of accuracy assessment (Congalton 1994) we consider the spatial accuracy of the maps. Whereas in the previous section only total area per class was taken into consideration, here we look at a pixel-per-pixel comparison of land-cover classes. This spatial analysis comparison is aimed at detecting inaccuracies more accurately.

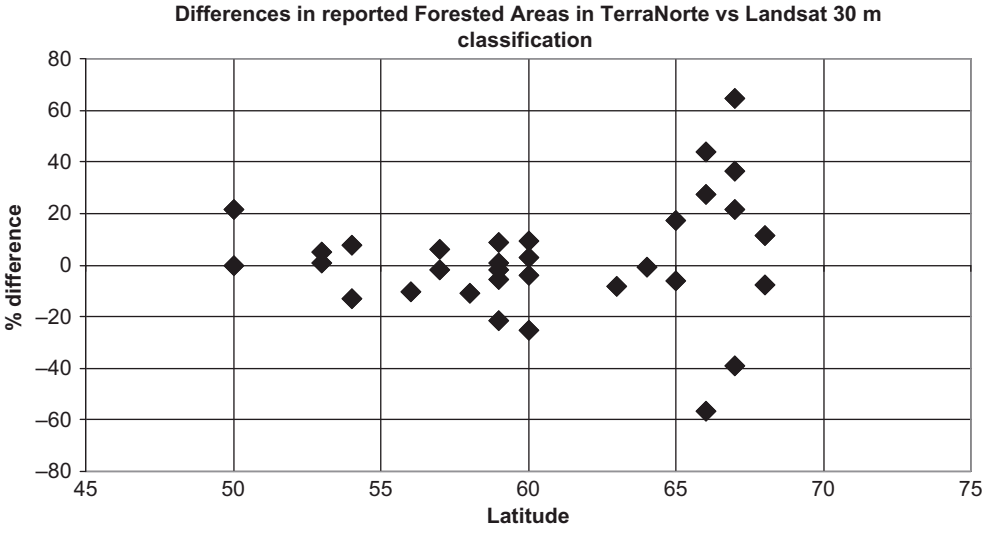

Figure 4. Relative differences between forest areas from TerraNorte map *versus* Landsat 30 m maps (Landsat 30 m maps used as reference).

Two classes are not reported in the confusion matrix, Recent burns and Water bodies, due to their limited area extent. These two classes are grouped within the class Other land (Table 5).

From this confusion matrix the overall accuracy (agreement between Landsat and TerraNorte maps) is 44%, with a kappa coefficient of 0.37 and a κ_{loc} coefficient of 0.41. The overall accuracy is rather low and may possibly reflect the selection of more classes than can be reasonably separated with the method and data used for the

Table 4. Coefficients of correlation between TerraNorte and 30 m resolution maps per land-cover class for regions below 65° N and above 65° N.

	Correlation	
Land-cover class	S of 65° N	N of 65° N
All forests	0.9999	0.7174
All broadleaf forests	0.9767	–0.0351
Deciduous broadleaf	0.9627	–0.0308
Mixed broadleaf majority 80%	0.8744	–0.1116
All needleleaf forests	0.9992	0.8480
Deciduous needleleaf forest	0.9978	0.8710
Sparse deciduous	0.9931	0.6419
Evergreen dark needleleaf forest	0.9877	0.9560
Evergreen light needleleaf forest	0.9923	1.0000
Mixed needleleaf majority 80%	0.9794	–0.1000
Mixed forests	0.9577	–0.1000
Other land	0.9962	–0.3532
Peatlands	0.9963	0.8850
Recent burns	0.9917	0.6397
Shrubs	0.9968	0.4427
Water bodies	0.9931	0.9602

Table 5. Confusion matrix between TerraNorte and 30 m resolution maps (areas in ha).

		TerraNorte map											
Classes (ha)		ED	EL	Brd	MNM	M	MBM	DN	SD	Shrubs	Ptlnd	Other land	% Agreement
Landsat classification	ED	63,165	5937	6711	16,745	5663	3623	9513	171	10	1919	3791	54
	EL	16,715	63,074	4691	15,260	5291	2022	14,078	375	12	14,473	8426	44
	Brd	1969	15,975	34,060	4278	8427	12,803	13,040	265	39	6719	17,848	30
	MNM	17,324	13,096	14,959	19,271	11,670	6808	8131	49	7	4157	3884	19
	M	5616	4373	25,393	5752	4547	7714	4514	99	6	3923	7445	7
	MBM	1211	1926	1200	1053	2100	1284	2235	12	2	344	1219	10
	DN	2867	4284	679	2315	5623	4400	148,791	18,351	25,486	7932	11,319	64
	SD	204	2324	163	188	559	1010	51,233	22,606	12,695	5559	3570	23
	Shrubs	2771	2	3003	426	267	243	6379	7378	15,652	20,237	4577	26
	Ptlnd	3404	14,491	1696	393	103	127	1886	6818	1151	77,149	8938	66
	Other land	4915	9973	12,073	2775	2839	2388	27,614	8952	3724	13,018	106,820	55
% Agreement		53	47	33	28	10	3	52	35	27	50	60	44.1

coarse-resolution map. Therefore we simulated a reduction in the number of classes by combining some. A generalized confusion matrix is generated by grouping the forest classes into broader categories (i.e. 'All needleleaf forests', 'All broadleaf forests', and 'Mixed forests' (Table 6)). The All needleleaf forests class includes the original classes Evergreen dark needleleaf forests, Evergreen light needleleaf forests, Deciduous needleleaf forests, Sparse deciduous forests, and Mixed needleleaf majority forests. The All broadleaf forests class includes Deciduous broadleaf forests and Mixed broadleaf majority forests. Water bodies and Recent burns were added to the Other land class as these classes are not the focus of this study. This generalized confusion matrix reports a higher accuracy of 61%, with a kappa coefficient of 0.41 and a κ_{loc} coefficient of 0.44.

Given the significant variation in correlations for regions above and below 65° N, confusion matrices are created for these two regions (Tables 7 and 8). Whereas the overall accuracy increases for both matrices, the kappa and κ_{loc} coefficients increase for the region below 65° N (to 0.43 and 0.46, respectively) but decrease for the region above 65° N (to 0.34 and 0.39 respectively).

4. Discussion

The levels of agreement between TerraNorte and Landsat-derived maps from the two types of analysis, correlation analysis, and spatial analysis allow us to analyse our results in a quantitative and objective manner.

The strong correlation between the Landsat-derived maps at 30 m resolution and the Landsat-derived maps resampled at 230 m indicates that such spatial thematic degradation (from 30 m to 230 m resolution) does not lead to a large loss of information at the site level for this boreal region (Table 2). Of course this does not refer to the loss of spatial detail from the increase in resolution. The spatially degraded Landsat maps (in contrast to the TerraNorte map) do not tend to under-represent small extents of classes within one site, nor to over-represent larger extents of classes. The discrepancies between Landsat-derived maps and the TerraNorte map may therefore be interpreted as a measure of the significant effect of the point spread function (PSF) of the MODIS sensor on land-cover characterization as reported by Huang et al. (2002). Their findings suggest that in order to achieve the desired performance level, land-cover products may need to be aggregated to coarser spatial resolutions.

Our results show clearly that smaller areas are generally under-represented in the TerraNorte map (Figure 3), which is in agreement with the findings of Lu et al. (2011). This is also in accordance with reported detection capabilities of MODIS for clear cuts in European Russia: below 10 ha size the detection of clear cuts becomes unreliable, approaching the level of single MODIS pixels and only above 15 ha does the detection become reliable and meaningful (Bucha and Stibig 2008). It is equally clear that for any given site, large patches tend to be over-represented (in terms of total area) when compared with the Landsat 30 m maps. This can be related to the heterogeneity of land-cover composition for pixels of 230 m × 230 m size. The spatial details of a 30 m × 30 m resolution map can get lost within 230 m × 230 m-sized pixels for complex landscapes. But given the high correlation between the degraded Landsat classification at 230 m resolution and the Landsat 30 m classification, the results from this study prove that the extraction of useful information from individual MODIS pixels is substantially inhibited by the contribution of surrounding pixels. This is in line with the reported modular transfer function effect on MODIS by Townshend et al. (2000) and the point spread function on land-cover characterization by MODIS reported by Huang et al. (2002).

Table 6. Confusion matrix between TerraNorte and 30 m resolution maps with simplified legend (areas in ha).

Land-cover classes		TerraNorte map						
		All needleleaf	All broadleaf	Mixed forest	Shrubs	Peatlands	Other land	% Agreement
Landsat map	All needleleaf	**516,067**	45,067	28,805	38,211	34,040	30,989	74
	All broadleaf	41,964	**49,346**	10,528	41	7062	19,067	39
	Mixed forest	20,354	33,107	**4547**	6	3923	7445	7
	Shrubs	16,956	3247	267	**15,652**	20,237	4577	26
	Peatlands	26,991	1823	103	1151	**77,149**	8938	66
	Other land	54,228	14,461	2839	3724	13,018	**106,820**	55
% Agreement		76	34	10	27	50	60	60.9

Note: Bold values highlight the values for the same classes in the Landsat Map and in the TN map.

Table 7. Confusion matrix between TerraNorte and 30 m resolution maps with simplified legend for region below 65° N. Areas in ha.

Land-cover classes		TerraNorte						
		All Needleleaf	All broadleaf	Mixed forest	Shrubs	Peatlands	Other land	% Agreement
Landsat map	All needleleaf	**325,631**	41,653	28,783	66	11,569	16,762	77
	All broadleaf	39,757	**48,910**	10,528	19	2089	17,456	41
	Mixed forest	19,866	33,107	4547	1	846	6994	7
	Shrubs	1823	1375	267	5	2219	1419	0
	Peatlands	12,497	164	103	16	**39,774**	4528	70
	Other land	37,373	12,826	2839	135	6906	**95,921**	61
% Agreement		75	35	10	2	63	67	62.1

Note: Bold values highlight the values for the same classes in the Landsat Map and in the TN map.

Table 8. Confusion matrix between TerraNorte and 30 m resolution maps with simplified legend for region above 65° N (areas in ha).

		TerraNorte map						
Classes ha		All needleleaf	All broadleaf	Mixed forest	Shrubs	Peatlands	Other land	% Agreement
Landsat Map	All needleleaf	**190,436**	3414	22	15,393	22,471	13,601	78
	All broadleaf	2208	**436**	0	26	4973	1597	5
	Mixed forest	488	0	**0**	5	3077	446	0
	Shrubs	14,981	1871	0	**7750**	17,911	2757	17
	Peatlands	14,494	1659	0	112	**37,375**	4318	64
	Other land	16,856	1635	0	1826	6112	**10,130**	28
% Agreement		80	5	0	31	41	31	61.8

Note: Bold values highlight the values for the same classes in the Landsat Map and in the TN map.

Table 9. Kappa and 'kappa location' results for all confusion matrices.

	$P(A)$	$P(E)$	P(max)	Kappa	Kappa location
Extended confusion matrix (Table 5)	44.06	11.66	89.91	0.37	0.41
Simplified CM (Table 6)	60.95	34.33	95.38	0.41	0.44
Simplified CM – region below 65° N (Table 7)	62.12	33.61	95.41	0.43	0.46
Simplified CM – region above 65° N (Table 8)	61.78	41.9	93.01	0.34	0.39

Sites having a correlation coefficient below 0.7 represent the most difficult and challenging cases for land-cover mapping. These sites are characterized by the most complex landscapes and the presence of land-cover types that are around the thresholds used for the definition of two or more classes. For example, the characterization of the different classes of Mixed forests with thresholds of 80% cover is challenging in the absence of detailed field information. Similarly, recent clear cuts can be mapped as shrubs when enough tree regrowth is present, when it corresponds in reality to young forest cover (Broadleaved forest). The correct labelling of forest regrowth is heavily dependent on the age of regrowth, light conditions, and influence of bare ground partially covering the area.

For the region above 65° N, the significant decrease in correlation between the two classifications is probably due to the dominance of more open forest stands and smaller trees, and thus the stronger disturbing effect of the bare component of the land areas. This is illustrated by the absence of correlation for the classes broadleaf forests, mixed forests, and other land. Although it could be argued that due to the rather restricted number of sample sites (11) for this area, further research is advisable to confirm these initial findings.

The spatial measures of agreement indicate clearly that both maps agree well for general classes (Table 9). It is only when trying to delineate more specific forest types that the maps diverge significantly. The land-cover maps under comparison are characterized by variation in spatial resolution. One TerraNorte pixel at 230 m × 230 m resolution will contain approximately 58 Landsat pixels at 30 m × 30 m resolution. Consequently the TerraNorte map should represent more consistently those land-cover classes with large and continuous coverage (through the selection of the dominant class in the classification process), whereas Landsat-based maps should represent more accurately those land-cover classes with more limited or fragmented coverage. This can explain both overlaps for classes with limited and fragmented spatial extent (e.g. Broadleaf forests, Mixed forest, and Other land), and the robustness of the needleleaf class that covers large homogeneous areas with fairly uniform spectral characteristics.

The needleleaf forests class is detected in a consistent manner and can be considered as a robust class in the TerraNorte map across the entire Russian territory – indeed, the producer's and user's accuracies are 76% and 74%, respectively. All other classes, however, with the possible exception of Peatlands, have a low detection rate above 65° N. The confusion matrix for the region above 65° N has a kappa of 0.34, which indicates only a fair agreement as seen from the lower correlation coefficients. For the region below 65° N the agreement is stronger and can be considered as moderate.

The confusion occurring between evergreen light needleleaf forests (EL) and deciduous broadleaf forests is a well-known problem (Bartalev 2006) and can be explained by the spectral similarity of the component of these two classes. There is also confusion between EL and Peatlands, which is explained by the fact that EL forests can grow on peatland soils and is an open canopy class. Broadleaf forest under boreal conditions

represents a challenge for accurate mapping, as these forest stands can be quite open and thus are more difficult to identify due to the higher contribution of the background to spectral reflectance. This explains the high level of confusion between Broadleaf forests and Other land. Another large part of the Broadleaf forests is confused with Mixed forests, which can further be explained by the spatial complexity of these classes. The accurate mapping of Mixed forests is therefore challenging, as expected, even at 30 m resolution. Another challenging class is Shrubs, which includes vegetation from 50 cm up to 5 m in height. The difficulty with this class relates to the fact that in boreal areas, Shrubs are mostly located in mountain and tundra areas.

The overall high correlations between the Landsat 30 m classification and the TerraNorte map for the combined class All forests (see also Figure 5) prompted us to calculate a forest area estimate for Russia by combining the TerraNorte map available for the entire Russian Federation and the sample of forest maps derived from Landsat imagery. A correction needs to be applied to the forest area measures from the TerraNorte map as there is an over-representation of large patches and an under-representation of small patches when compared with reference maps. Based on approaches used by Potapov et al. (2008) and by Stehman, Sohl, and Loveland (2003), the correction is done by determining and applying three linear regression equations to the All forest class areas: for the full territory and both above and below 65° N (Tables 10 and 11; Figure 5). The resulting estimate (823.0 ± 58.2 million ha) compares well to the figure from the FAO Forest Resource Assessment 2010 (814.7 million ha; FAO 2010), which is derived from the national forest inventory, with a 1% relative difference in mean estimate.

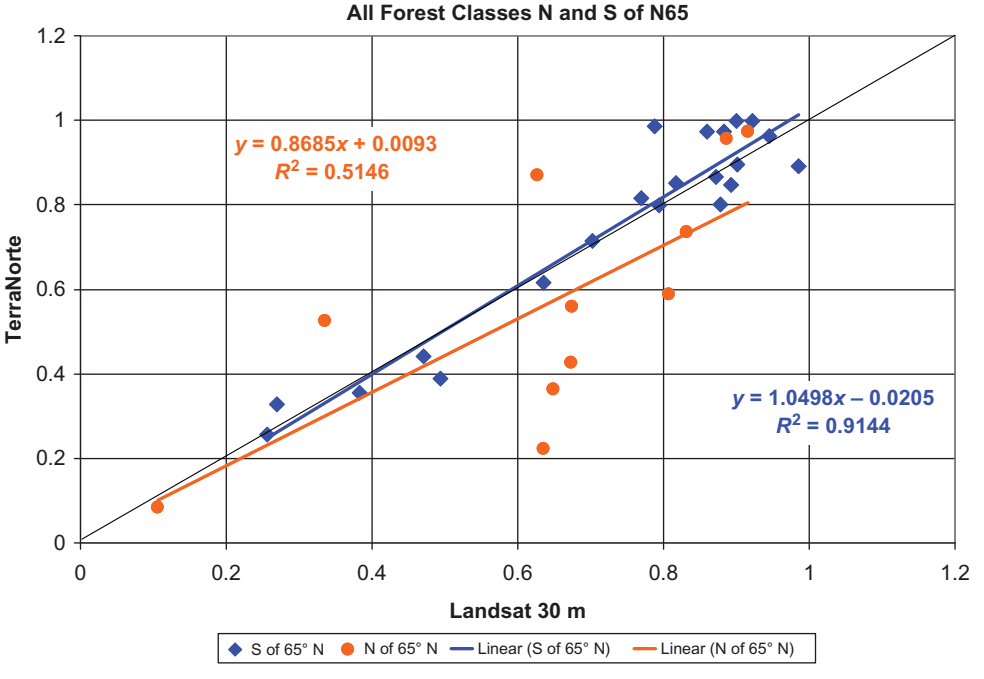

Figure 5. Linear regressions of forest percentages within sample sites between TerraNorte map and Landsat 30 m maps for regions below and above 65° N.

Table 10. Linear regressions for forest area estimates.

Nb	Region	Linear regression	Correlation coefficient (r)	Standard error (%)
1	Whole Russia	$y = 1.0187 \times - 0.0288$	0.86	14.04
2	Region below 65° N	$y = 1.0498 \times - 0.0205$	0.72	7.44
3	Region above 65° N	$y = 0.8685 \times + 0.0093$	0.96	21.43

Table 11. Estimates of forest areas (ha) for the Russian Federation.

Forest area (ha)	TerraNorte	Landsat corrected	Standard error
From regression 1 for whole Russia	**807,664,282**	**822,766,451**	**115,516,410**
From regression 2 (below 65° N)	670,281,575	703,660,778	52,352,362
From regression 3 (above 65° N)	137,382,707	119,317,252	25,569,687
Whole Russia (Sum 2 + 3)	**807,664,282**	**822,978,030**	**58,263,013**

Note: Bold values highlight the values for the same classes in the Landsat Map and in the TN map.

5. Conclusions

Differences between two land-cover mapping initiatives (TerraNorte map and reference forest maps derived from Landsat TM imagery) have been assessed through quantitative and spatial analyses. The land-cover initiatives were very similar in that they covered the same time window (the year 2010) and used the same land-cover legend. They differed in the resolution of their input data (230 m × 230 m and 30 m × 30 m, respectively).

The quantification of the agreement was principally based on cross-tabulations of the map legends using standard measures as the kappa coefficient to infer a degree of difference. General vegetation classes (e.g. All forests and Needleleaf forests) can be well detected and show high areal and moderate spatial correlation agreements. On the other hand, accurate mapping from moderate-resolution imagery of more specific forest cover classes remains more challenging, especially for northern latitudes where forest canopy cover is more open and spectral reflectances are influenced by background cover.

The coarse-scale TerraNorte land-cover map corresponds well with the reference forest maps derived from Landsat imagery when considering area estimates for main forest cover types. It does show some discrepancies when compared to reference forest maps derived from Landsat imagery when looking at more detailed land-cover types. The impact of over- and under-representation of land-cover classes in the moderate-resolution map is quantified. As reported by Townshend et al. (2000), such impact can disappear for large regions due to a compensation effect. In this study we indicate that over- and under-representation are important factors when using more detailed forest-cover classes. One has to be careful when considering the thematic information from individual coarse-resolution pixels. The effective point spread function needs to be quantified to infer a correct indication of the spatial accuracy that can be obtained for final products, as indicated by Huang et al. (2002).

We report a total forest area estimation for the Russian Federation, which corresponds well to the national Russian estimate. We can thus conclude that such a coarse-resolution map, with the addition of a sample of reference maps, can complement estimates of the national forest inventory by providing a spatial component available for the full territory. Based on this study we can expect that the next generation of Vegetation instruments will

allow the production of coarse-resolution scale maps suitable for forestry applications in boreal ecosystems.

References

Achard, F., H. D. Eva, D. Mollicone, and R. Beuchle. 2008. "The Effect of Climate Anomalies and Human Ignition Factor on Wildfires in Russian Boreal Forests." *Philosophical Transactions of the Royal Society B* 363: 2331–2339.

Achard, F., D. Mollicone, and H. J. Stibig. 2006. "Areas of Rapid Forest-Cover Change in Boreal Eurasia." *Forest Ecology and Management* 237: 322–334.

Arino, O., P. Bicheron, F. Achard, J. Latham, R. Witt, and J. L. Weber. 2008. "The Most Detailed Portrait of Earth." *European Space Agency Bulletin* 136: 24–31.

Bartalev, S. S. 2006. "Development of Sensing Methods for Regional Ecological Assessment of Forest Cover." PhD thesis, 130pp. [in Russian].

Bartalev, S. A., F. Achard, V. A. Egorov, S. Khvotikov, N. Kuzmenko, S. S. Bartalev, and O. Kissiyar. 2012. "Evaluation of Impact of Enhanced Spatial Resolution (Proba-V vs. Vegetation) for Land Cover Mapping Accuracy over Russia Final Report to Proba-V Preparatory Programme." Space Application Institute of Russian Academy of Science, Moscow, Russia, 47p.

Bartalev, S. A., V. A. Egorov, D. V. Ershov, A. S. Isaev, E. A. Loupian, D. E. Plotnikov, and I. A. Uvarov. 2011. "The Vegetation Mapping over Russia Using MODIS Spectroradiometer Satellite Data." *Contemporary Earth Remote Sensing From Space* 8: 285–302 [in Russian].

Bartalev, S. A., D. Erchov, A. Isaev, and A. Belward. 2003. "A New SPOT4-Vegetation Derived Land-Cover Map of Northern Eurasia." *International Journal of Remote Sensing* 24: 1977–1982.

Bartholomé, E., and A. S. Belward. 2005. "GLC2000: A New Approach to Global Land Cover Mapping from Earth Observation Data." *International Journal of Remote Sensing* 26: 1959–1977.

Beuchle, R., H. Eva, H. J. Stibig, C. Bodart, A. Brink, P. Mayaux, D. Johansson, F. Achard, and A. S. Belward. 2011. "A Satellite Data Set for Tropical Forest Area Change Assessment." *International Journal of Remote Sensing* 32: 7009–7031.

Bodart, C., H. R. Eva, R. Beuchle, R. Raši, D. Simonetti, H. J. Stibig, A. Brink, E. Lindquist, and F. Achard. 2011. "Pre-Processing of a Sample of Multi-Scene and Multi-Date Landsat Imagery Used to Monitor Forest Cover Changes over the Tropics." *ISPRS Journal of Photogrammetry and Remote Sensing* 66: 555–563.

Broich, M., M. C. Hansen, P. Potapov, A. Adusei, E. Lindquist, and S. V. Stehman. 2011. "Time-Series Analysis of Multi-Resolution Optical Imagery for Quantifying Forest Cover Loss in Sumatra and Kalimantan, Indonesia." *International Journal of Applied Earth Observation and Geoinformation* 13: 227–291.

Bucha, T., and H. J. Stibig. 2008. "Analysis of MODIS Imagery for Detection of Clear Cuts in the Boreal Forest in North-West Russia." *Remote Sensing of Environment* 112: 2416–2429.

Chavez, P. S., Jr. 1996. "Image-Based Atmospheric Corrections – Revisited and Improved." *Photogrammetric Engineering and Remote Sensing* 62: 1025–1036.

Congalton, R. G. 1994. "Accuracy Assessment of Remotely Sensed Data: Future Needs and Directions." In *Proceedings of Pecora 12 Land Information from Space-Based Systems*, 383–388. Bethesda, MD: ASPRS.

ESA. 2012. "PROBA-V Website." Accessed August 17, 2012. http://www.esa.int/esaMI/Proba/SEM9FS4PVFG_0.html

Eva, H. D., F. Achard, R. Beuchle, E. De Miranda, S. Carboni, R. Seliger, M. Vollmar, W. Holler, O. Oshiro, V. Barrena, and J. Gallego. 2012. "Forest Cover Changes in Tropical South and Central America from 1990 to 2005 and Related Carbon Emissions and Removals." *Remote Sensing* 4: 1369–1391.

FAO. 2010. *Global Forest Resources Assessment 2010: Main Report*. FAO Forestry Paper 163. ISBN 978-92-5-106654-6.

FAO & JRC. 2012. *Global Forest Land-Use Change 1990–2005*. FAO Forestry Paper No. 169. Rome: FAO, 40p. http://www.fao.org/forestry/fra/remotesensingsurvey/en/

Foody, G. M. 2002. "Status of Land Cover Classification Accuracy Assessment." *Remote Sensing of Environment* 80: 185–201.

Foody, G. M. 2010. "Assessing the Accuracy of Land Cover Change with Imperfect Ground Reference Data." *Remote Sensing of Environment* 114: 2271–2285.

Friedl, M. A., D. K. McIver, and J. C. F. Hodges. 2002. "Global Land Cover Mapping from MODIS: Algorithms and Early Results." *Remote Sensing of Environment* 83: 287–302.

Friedl, M. A., D. Sulla-Menashe, and B. Tan. 2010. "MODIS Collection 5 Global Land Cover: Algorithm Refinements and Characterization of New Datasets." *Remote Sensing of Environment* 114: 168–182.

Giri, C., Z. Zhu, and B. Reed. 2005. "A Comparative Analysis of the Global Land Cover 2000 and MODIS Land Cover Data Sets." *Remote Sensing of Environment* 94: 123–132.

Hansen, M. C., and B. Reed. 2000. "A Comparison of the IGBP DISCover and University of Maryland 1km Global Land Cover Products." *International Journal of Remote Sensing* 21: 1365–1373.

Hansen, M. C., J. Townshend, R. S. DeFries, and M. Carroll. 2005. "Estimation of Tree Cover Using MODIS Data at Global, Continental and Regional/Local Scales." *International Journal of Remote Sensing* 26: 4359–4380.

Huang, C., J. R. G. Townshend, S. Liang, S. N. V. Kalluri, and R. S. DeFries. 2002. "Impact of Sensor's Point Spread Function on Land Cover Characterization: Assessment and Deconvolution." *Remote Sensing of Environment* 80: 203–212.

Jensen, J. R. 1996. *Introductory Digital Image Processing: A Remote Sensing Perspective*. 2nd ed. Upper Saddle River, NJ: Prentice Hall.

Lu, D., M. Batistella, E. Moran, S. Hetrick, D. Alves, and E. Brondizio. 2011. "Fractional Forest Cover Mapping in the Brazilian Amazon with a Combination of MODIS and TM Images." *International Journal of Remote Sensing* 32: 7131–7149.

McCallum, I., M. Obersteiner, S. Nilsson, and A. Shvidenko. 2006. "A Spatial Comparison of Four Satellite Derived 1 Km Global Land Cover Datasets." *International Journal of Applied Earth Observation and Geoinformation* 8: 246–255.

Pontius, R. G., Jr. 2000. "Quantification Error versus Location Error in Comparison of Categorical Maps." *Photogrammetric Engineering & Remote Sensing* 66: 1011–1016.

Potapov, P., M. C. Hansen, S. V. Stehman, T. R. Loveland, and K. Pittman. 2008. "Combining MODIS and Landsat Imagery to Estimate and Map Boreal Forest Cover Loss." *Remote Sensing of Environment* 112: 3708–3719.

Reese, H. M., T. M. Lillesand, D. E. Nagel, J. S. Stewart, R. A. Goldmann, T. E. Simmons, J. W. Chipman, and P. A. Tessar. 2002. "Statewide Land Cover Derived from Multiseasonal Landsat TM Data, a Retrospective of the WISCLAND Project." *Remote Sensing of Environment* 82: 224–237.

Richards, T. S., J. Gallego, and F. Achard. 2000. "Sampling for Forest Cover Change Assessment at the Pan-Tropical Scale." *International Journal of Remote Sensing* 21: 1473–1490.

Stehman, S. V. 2001. "Statistical Rigor and Practical Utility in Thematic Map Accuracy Assessment." *Photogrammetric Engineering and Remote Sensing* 67: 727–734.

Stehman, S. V., M. C. Hansen, M. Broich, and P. V. Potapov. 2011. "Adapting a Global Stratified Random Sample for Regional Estimation of Forest Cover Change Derived from Satellite Imagery." *Remote Sensing of Environment* 115: 650–658.

Stehman, S. V., T. L. Sohl, and T. R. Loveland. 2003. "Statistical Sampling to Characterize Recent United States Land Cover Change." *Remote Sensing of Environment* 86: 517–529.

Stehman, S. V., J. D. Wickham, J. H. Smith, and L. Yang. 2003. "Thematic Accuracy of the 1992 National Land-Cover Data for the Eastern United States: Statistical Methodology and Regional Results." *Remote Sensing of Environment* 86: 500–516.

Townshend, J. R. G., C. Huang, S. N. V. Kalluri, R. S. Defries, and S. Liang. 2000. "Beware of per Pixel Characterization of Land-Cover." *International Journal of Remote Sensing* 21: 839–843.

Uvarov, I., and S. A. Bartalev. 2010. "Algorithm and Software Suite for Land Cover Types Recognition Based on Locally-Adaptive Supervised Classification of Satellite Imagery." In *Proceedings of Contemporary Remote Sensing from Space: Physical Background*, *Methods and Technologies for Environmental Monitoring*, Moscow, 7, 353–365 [in Russian].

Weber, K. T. 2006. "Challenges of Integrating Geospatial Technologies into Rangeland Research and Management." *Rangeland Ecological Management* 59: 38–43.

Xie, Y., Z. Sha, and M. Yu. 2008. "Remote Sensing Imagery in Vegetation Mapping: A Review." *Journal of Plant Ecology* 1: 9–23.